Supplementary Materials

Efficient Triplet-Triplet Energy Transfer Activating Room-Temperature Phosphorescence of Coumarin Guests

Mingyue Dong, [a] Hua Feng, [a] Wanjuan Gao, [a] Dan Li, [*a] Fushun Liang, [*c] Lili Wen [a]& Zhongmin Su [*a, b]

a Jilin Provincial Science and Technology Innovation Center of Optical Materials and Chemistry, Jilin Provincial International Joint Research Center of Photo-functional Materials and Chemistry, School of Chemistry and Environment, Changchun University of Science and Technology, Changchun, 130022, China

b State Key Laboratory of Supramolecular Structure and Materials, College of Chemistry, Jilin University, Changchun, 130021, China

c College of Chemistry, Liaoning University, Shenyang, 110036, China

1. Experimental part

1.1 Reagent and material preparation

Since the materials obtained directly through commercial purchase are usually sensitive to impurities, the main and guest compounds used in the experiment were purified through three rounds of recrystallization, and the guest compounds were also subjected to nuclear magnetic resonance characterization (Figure S1-3).

Take 20 mg of CCA and add 4 mL of ethanol to a clean flask. Stir thoroughly to dissolve it until it becomes clear and transparent. Then, you will obtain a 5 mg/mL CCA-ethanol mixed solution.

Take CCA/IPA as an example: Take 0.3 g of IPA in a clean flask, add 6 mL of methanol, and then add a certain amount of 5 mg/mL CCA-ethanol mixed solution at different molar ratios. Stir thoroughly to dissolve until it becomes clear and transparent. The CCA/IPA materials with different doping concentrations can be prepared by vacuum rotary evaporation method.

The solid materials with other doping concentrations can be obtained through similar steps.

1.2 Measurement

Steady-state photoluminescence spectra, phosphorescence spectra, and phosphorescence decay curves under ambient conditions were measured with an FL-7100 spectrometer. Phosphorescence

spectra were acquired with a delay time of 8 ms. Phosphorescence spectra were measured using Edinburgh FLS1000 at 77 K. Photoluminescence quantum yields were collected for all materials under ambient conditions using an Edinburgh FLS 1000 equipped with an integrating sphere. Photoluminescence photos were taken with an iPhone XR under room temperature with handheld UV lamp (365 nm) illumination.

Powder x-ray diffraction (P-XRD) spectra were measured using a Shimadzu-6100 x-ray diffractometer with *Cu-Kα* radiation at a wavelength of 1.542 Å. Diffraction was measured over a 2θ angle range of 5-60° and recorded at a scan rate of 1 degree per minute.

The solid-state UV-visible absorption (UV-vis) spectra were obtained using Perkin Elmer Lambda35. The liquid-state UV-visible absorption spectra were obtained using UV- 5500 (PC).

Fourier-transform infrared spectroscopy (FT-IR) spectra were performed compound in the range of 4000-400 cm^{-1} on a Thermo Fisher FT-IR spectrophotometer (Nicolet iS50).

1.3 Calculation of the photophysical parameters

The phosphorescence quantum yields of the compounds were obtained from the following equation:

$$\phi_{Ph} = \frac{A_{Ph}}{A_{PL}} \times \phi_{PL}$$

where A_{PL} and A_{Ph} represent the integration regions of the total photoluminescence and phosphorescence spectra, respectively.

According to the reported literature, the energy gap (ΔE_{ST}) between the T_1 and S_1 was calculated by the following formula:

$$\Delta E_{ST} = hk(\frac{c}{\lambda_1} - \frac{c}{\lambda_2})$$

where the h is Planck constant (4.14×10^{-15} eV·s), c is velocity of light (3×10^{17} nm/s), k is conversion constant (1.6×10^{-19} J/eV), and λ_1 and λ_2 represent the fluorescence emission wavelength and phosphorescence emission wavelength respectively.

1.4 Theoretical calculation

For the theoretical simulations, the geometry of the ground state in the isolated state was fully optimized with density functional theory (DFT) with B3LYP hybrid functional at the basis set levels of 6-31G (d, p). All the excited state geometries were optimized by the time dependent DFT

(TD-DFT) with B3LYP functional at the same basis set level as the ground state. The excitation energies in the singlet (Sn) and triplet (Tn) states were obtained using TD-DFT method of td-tzvp wb97x. The spin-orbit coupling (SOC) was used to calculate SOC constants between singlet and triplet states, including both ground and excited states. Except for SOC calculations, which were conducted using the BDF method, the remainder of the computations were carried out with Gaussian 16 revision A.03.

2. Other properties

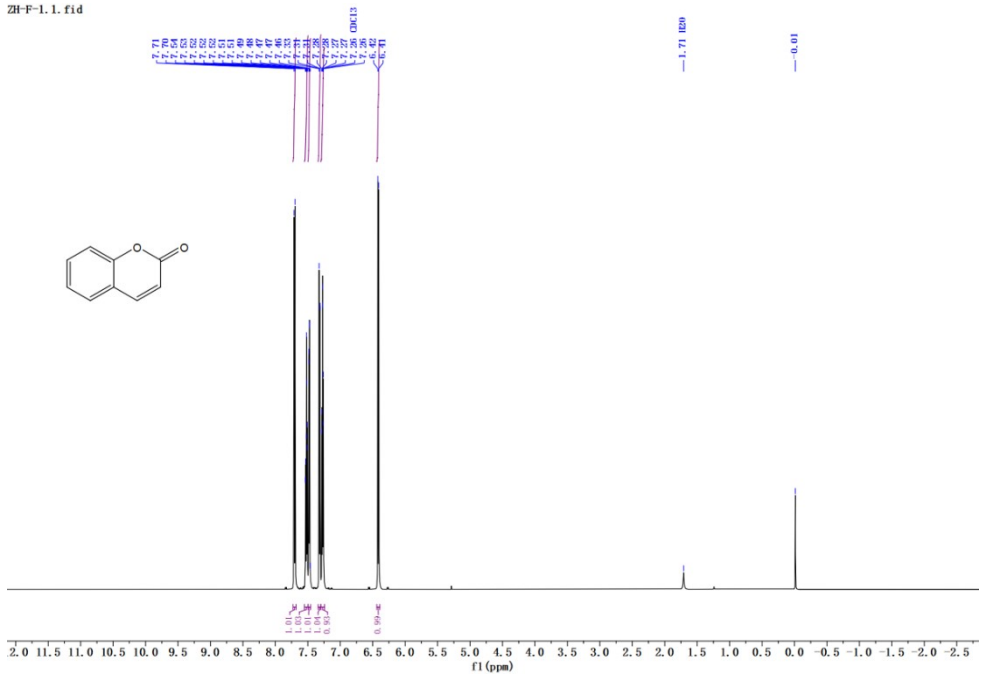

Figure S1. ^{1}H NMR spectra of C solid after three times of recrystallization.

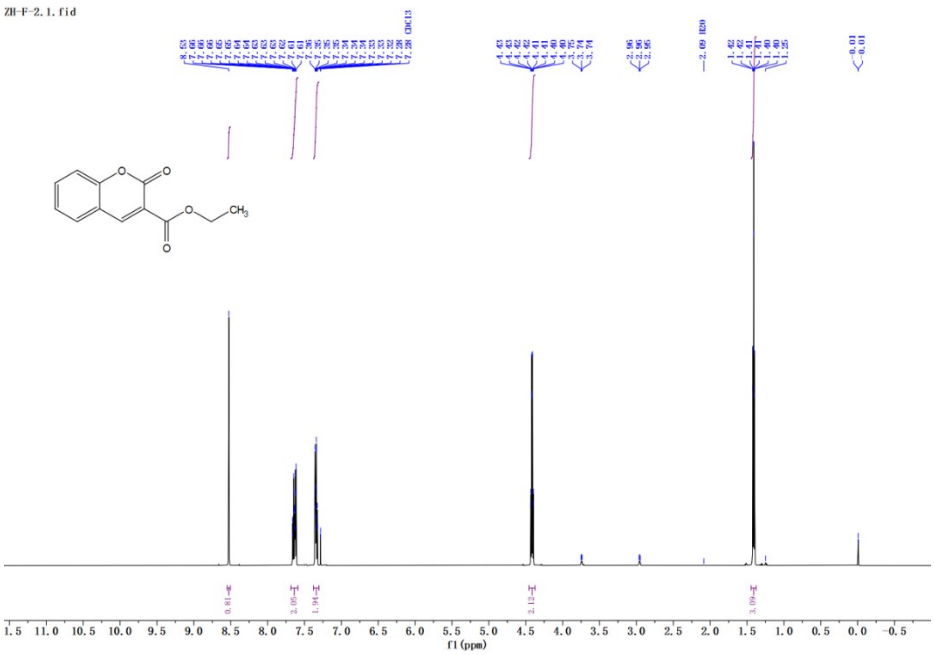

Figure S2. [1]H NMR spectra of CE solid after three times of recrystallization.

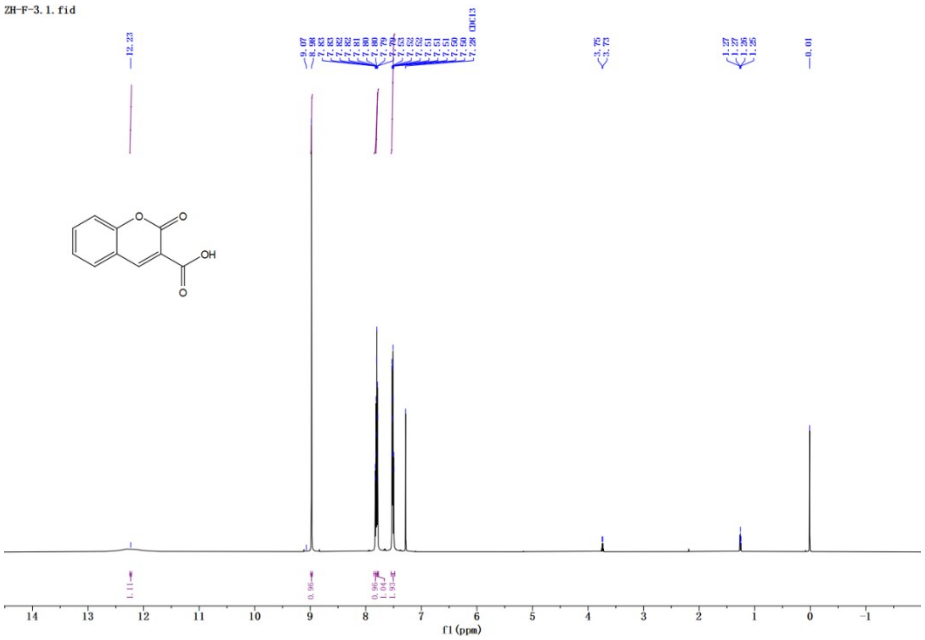

Figure S3. [1]H NMR spectra of CCA solid after three times of recrystallization.

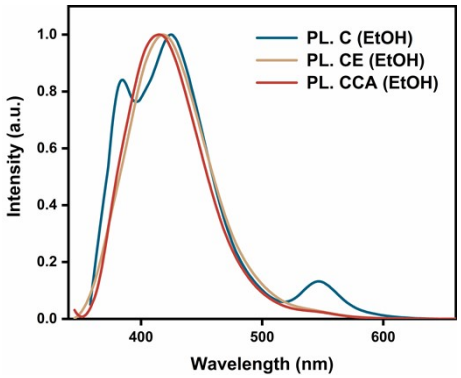

Figure S4. The steady-state PL spectrum of C/CE/CCA (1×10^{-5} M) at 298K (λ_{ex} = 348/325/341, Delay time = 8 ms).

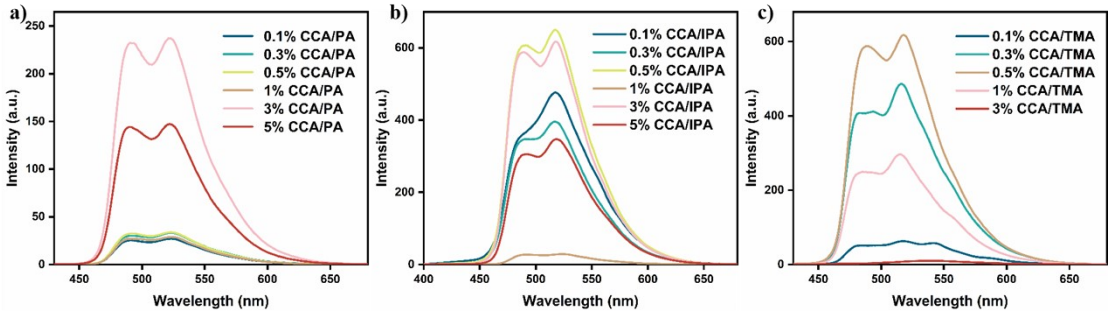

Figure S5. Delayed spectra of CCA dopants (0.1 mol%−5 mol%) in a) PA, b) IPA, c) TMA at 298 K (λ_{ex} = 365 nm, delayed time = 8 ms).

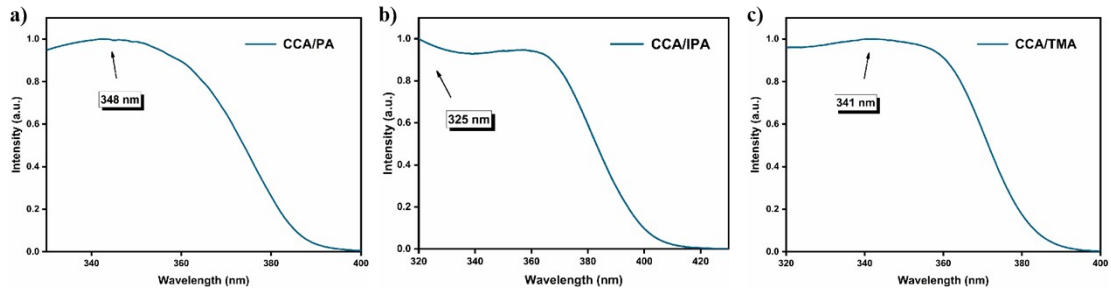

Figure S6. Excitation spectra of CCA/PA, CCA/IPA, and CCA/TMA solid at 298 K.

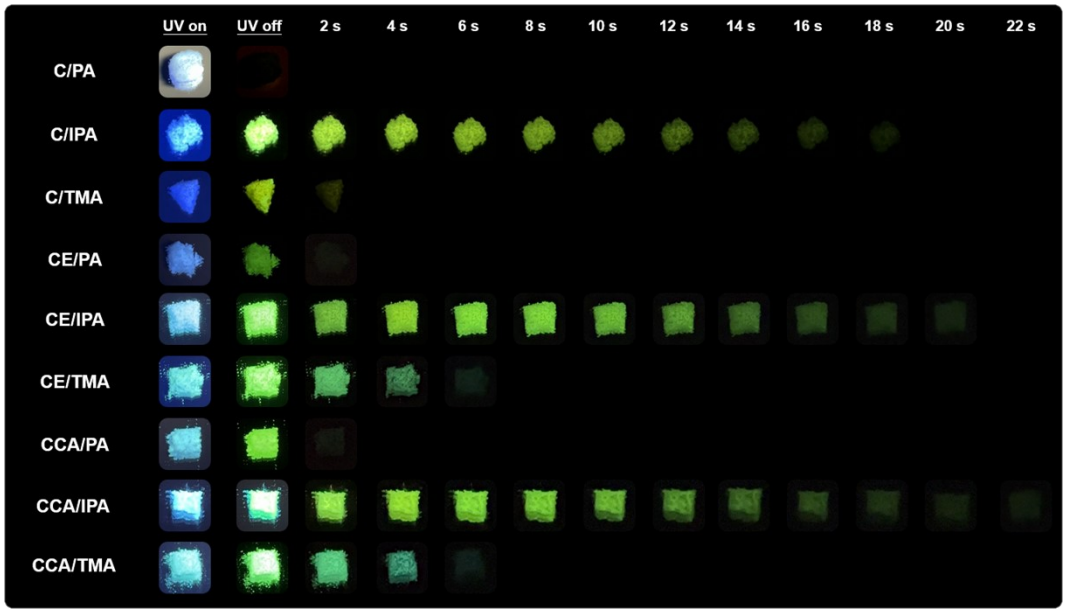

Figure S7. Fluorescence and phosphorescence emission photographs of Cums/Ar-COOH under 365 nm UV excitation.

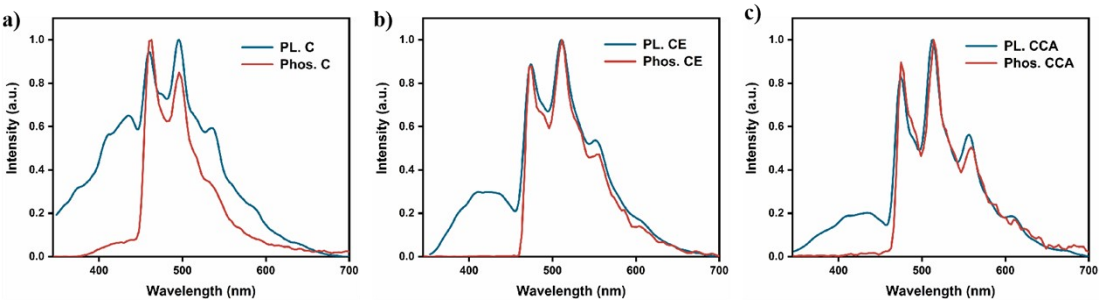

Figure S8. Steady-state PL spectra and phosphorescence spectra of a) C, b) CE, and c) CCA in ethanol solution (1×10^{-5} M) at 77 K

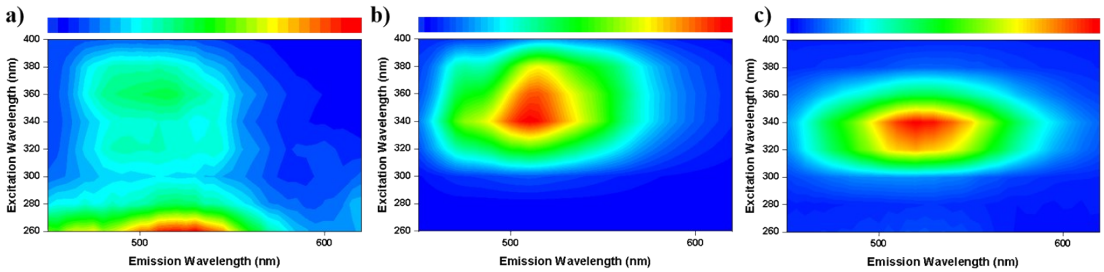

Figure S9. Excitation-phosphorescence emission mapping of a) PA, b) IPA, and c) TMA under ambient conditions.

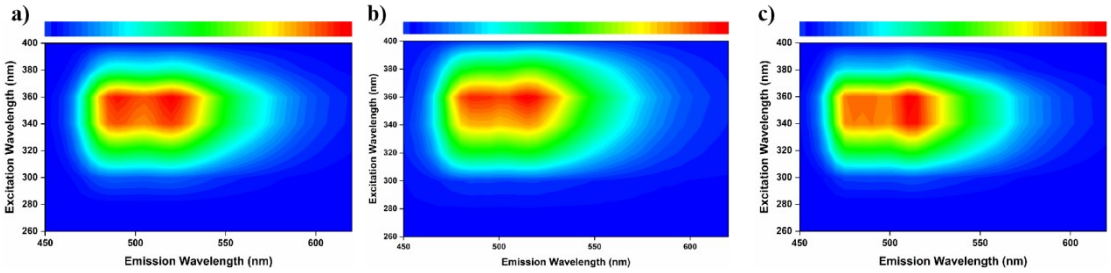

Figure S10. Excitation-phosphorescence emission mapping of a) CCA/PA, b) CCA@IPA and c) CCA/TMA under ambient conditions.

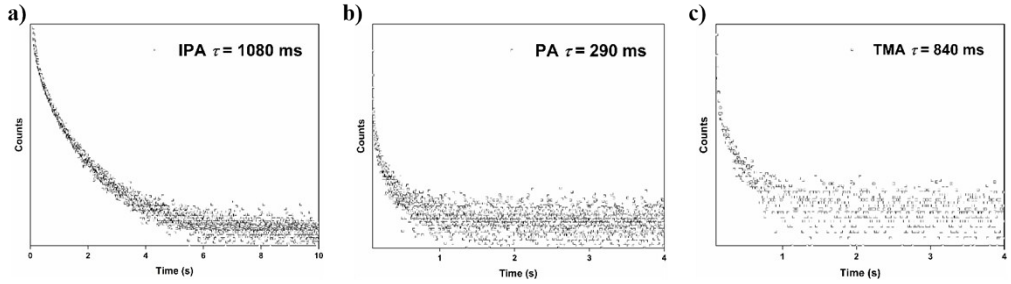

Figure S11. Phosphorescence decay curves of a) PA, b) IPA, and c) TMA solid at 298 K.

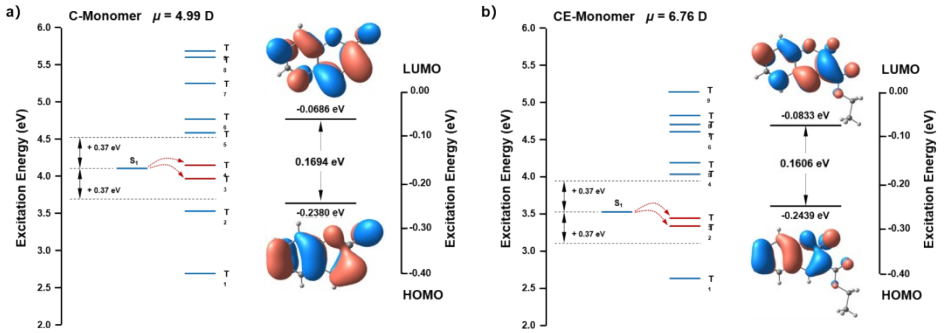

Figure S12. Theoretical calculation of dipole moment, energy level diagram, spin-orbit coupling (SOC) value (ξ), the highest occupied and lowest unoccupied molecular orbitals (HOMO, LUMO) of C and CE.

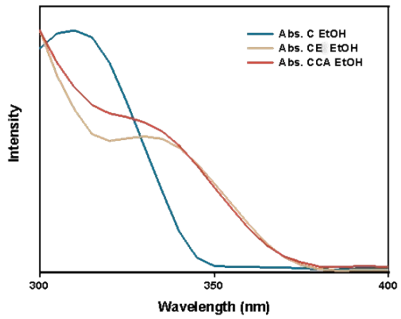

Figure S13. UV-visible absorption spectra of C, CCA, and CE in ethanol solution (1×10^{-5} M).

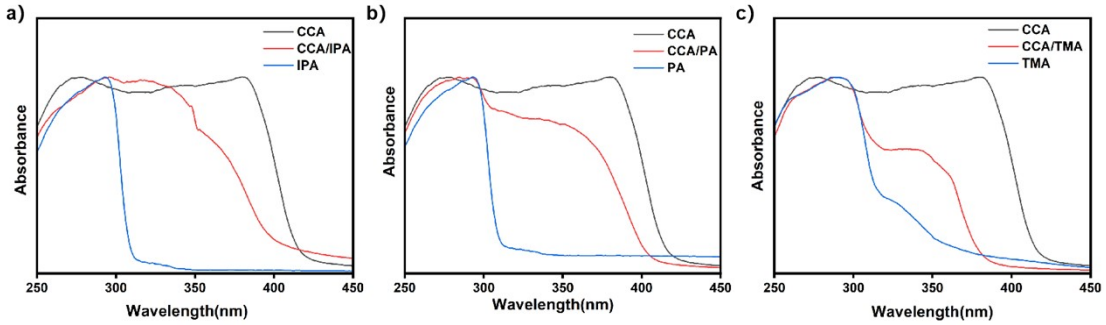

Figure S14. UV-visible absorption spectra of a) CCA, IPA and CCA/IPA solid, b) CCA, PA and CCA/PA solid and CCA, TMA and CCA/TMA solid.

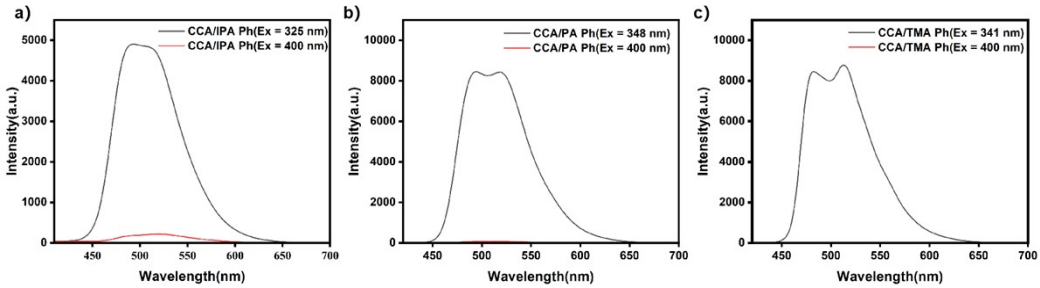

Figure S15. Phosphorescence spectra under different excitation wavelengths a) CCA/IPA, b) CCA/PA and c) CCA/TMA.

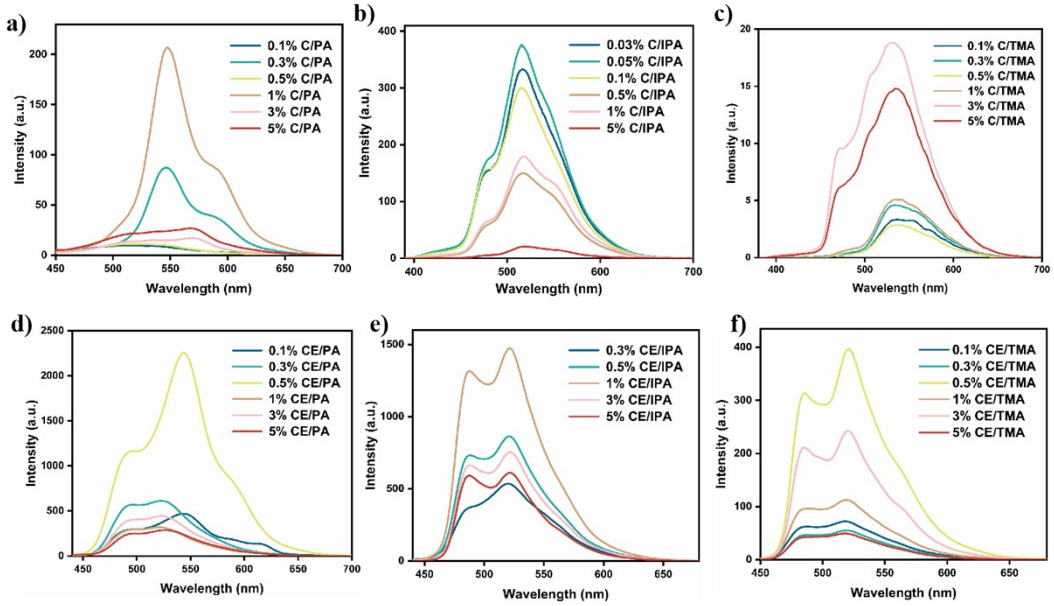

Figure S16. a-c) Delayed spectra of C dopants (0.1 mol%−5 mol%) in PA, IPA, TMA at 298 K (λ_{ex} = 365 nm, delayed time = 8 ms) d-f) Delayed spectra of CE dopants (0.1 mol%−5 mol%) in PA, IPA, TMA at 298 K (λ_{ex} = 365 nm, delayed time = 8 ms).

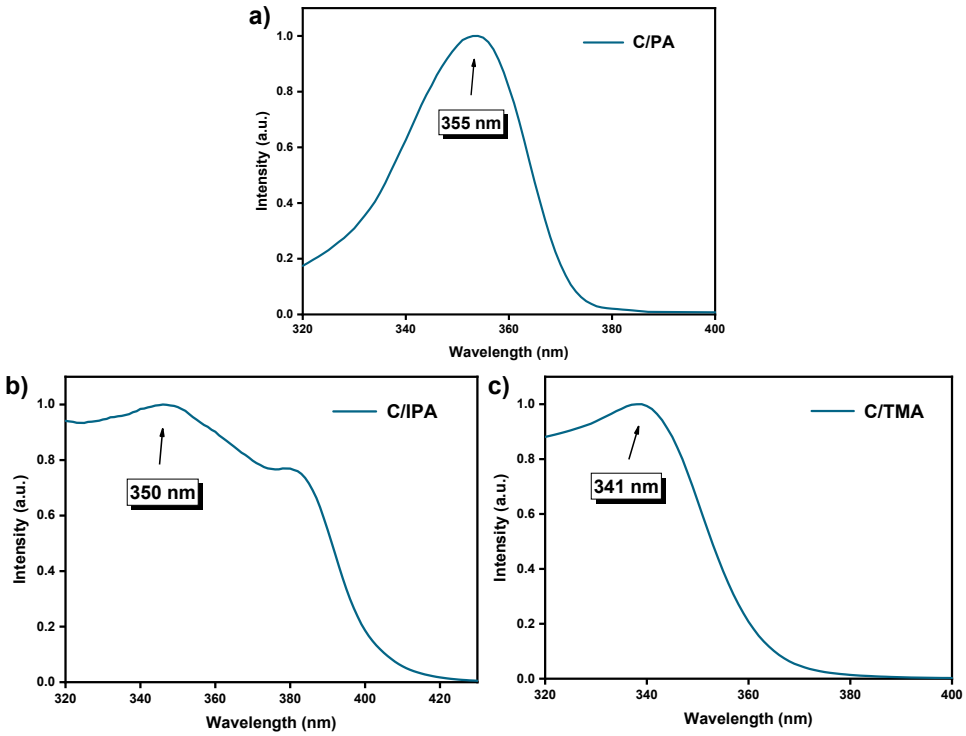

Figure S17. Excitation spectra of a) C/PA, b) C/IPA, and c) C/TMA solid at 298 K.

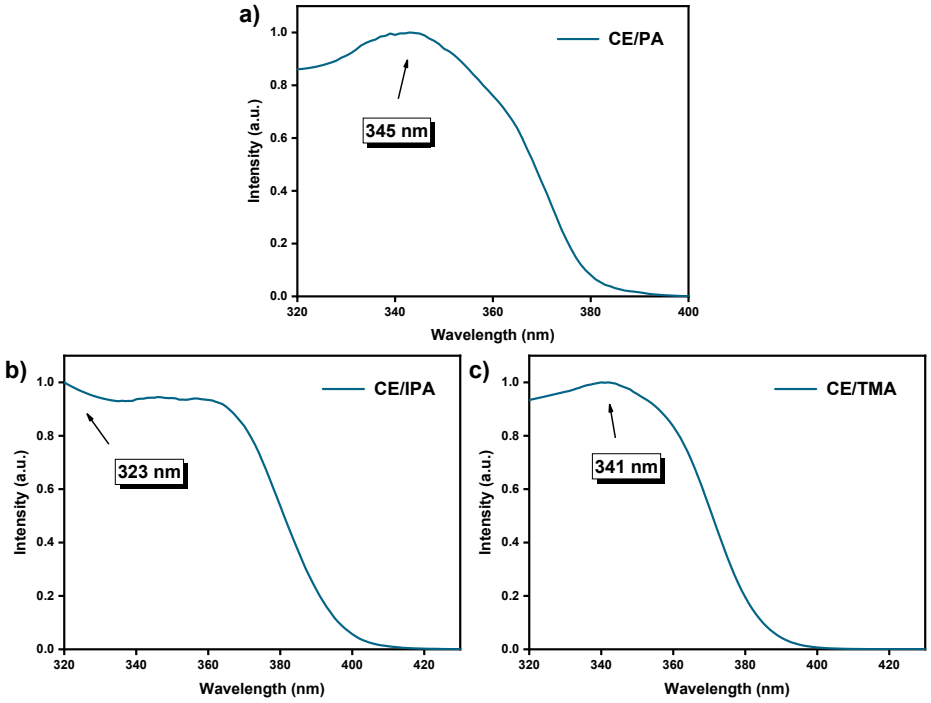

Figure S18. Excitation spectra of a) CE/PA, b) CE/IPA, and c) CE/TMA solid at 298 K.

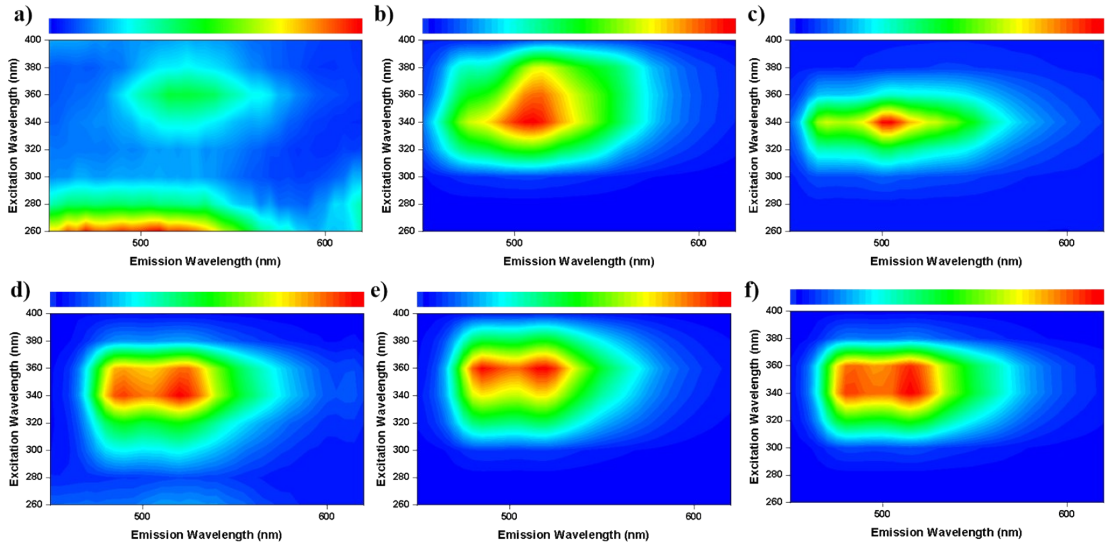

Figure S19. a-c) Excitation-phosphorescence emission mapping of C/PA, C/IPA, and C/TMA under ambient conditions d-f) Excitation-phosphorescence emission mapping of CE/PA, CE/IPA, and CE/TMA under ambient conditions.

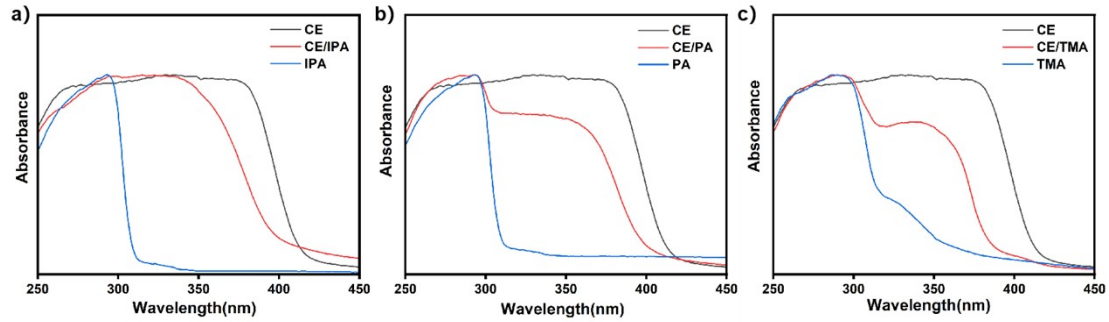

Figure S20. UV-visible absorption spectra of a) CE, IPA, CE/IPA b) CE, PA and CE/PA c) CE, TMA and CE/TMA.

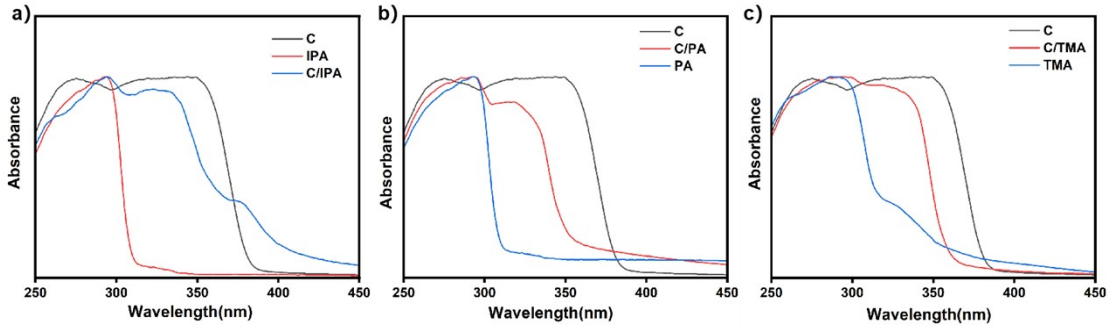

Figure S21. UV-visible absorption spectra of a) C, IPA, C/IPA b) C, PA and C/PA c) C, TMA and C/TMA.

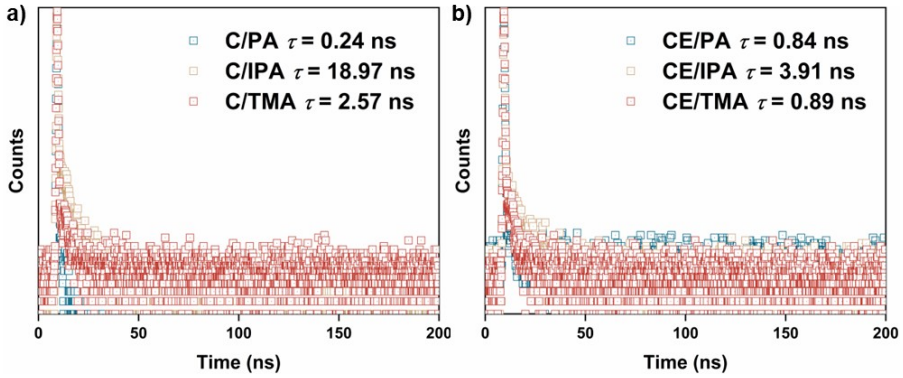

Figure S22. Fluorescence decay curves of a) C/Ar-COOH and b) CE/Ar-COOH (λ_{ex} = 450 nm)

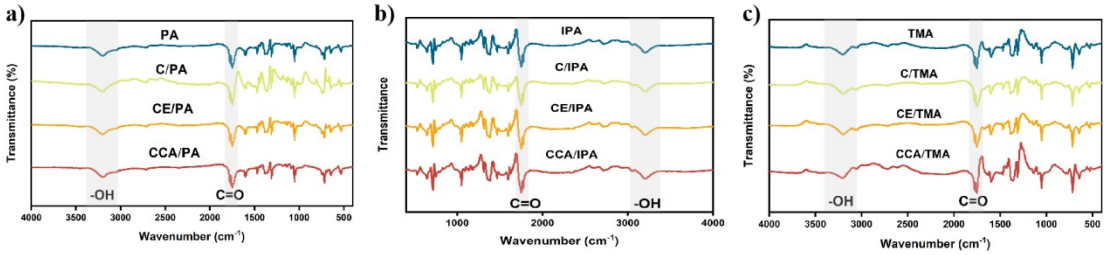

Figure S23. Fourier-transform infrared spectroscopy spectra of a) PA and Cums/PA, b) IPA and Cums/IPA, c) TMA and Cums/TMA

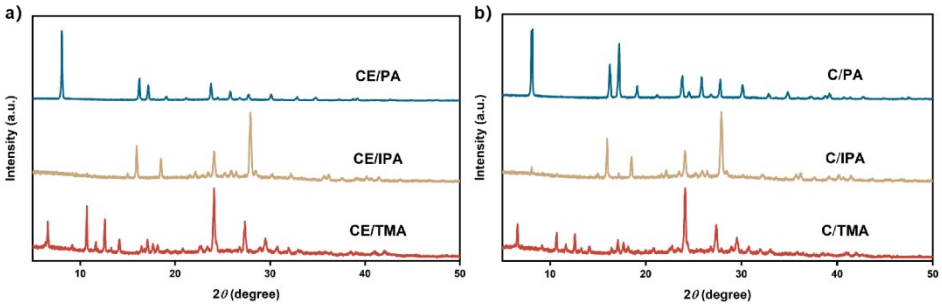

Figure S24. Powder X-ray diffraction (PXRD) patterns of, doped material a) CE/PA, CE/IPA, and CE/TMA; b) C/PA, C/IPA, and C/TMA

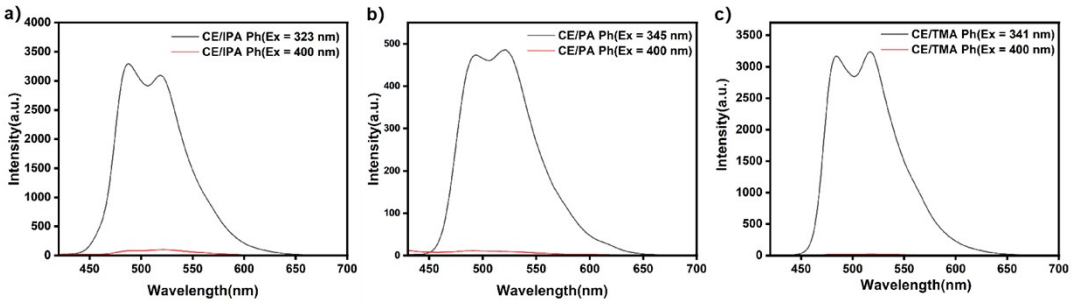

Figure S25. Phosphorescence spectra under different excitation wavelengths a) CE/IPA, b) CE/PA and c) CE/TMA.

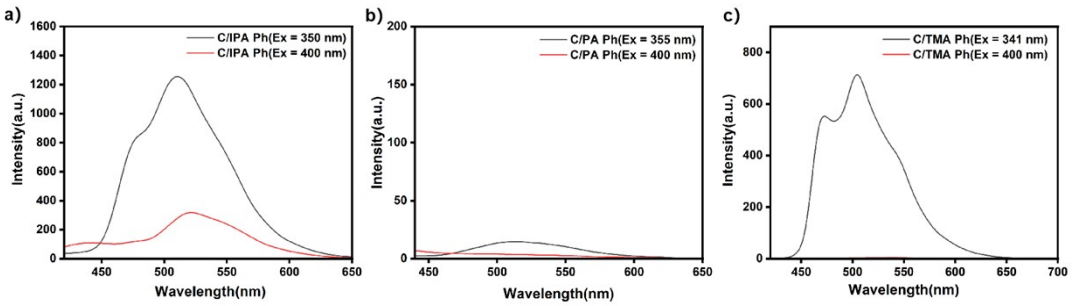

Figure S26. Phosphorescence spectra under different excitation wavelengths a) C/IPA, b) C/PA and c) C/TMA.

Table S1. Photophysical data of host (PA, IPA and TMA), guest (C,CCA and CE), and doped materials.

Sample [a]	λ_F [b](nm)	ϕ_F [c] (%)	λ_P [d] (nm)	τ_p [e] (ms)	ϕ_p [f] (%)	ϕ_{PL} [g](%)	k_p [i] (s^{-1})	k_{nr} [j] (s^{-1})
PA	418	2.45	497	290	0.88	3.33	3.03×10^{-2}	3.42×10^{0}
IPA	393	21.84	514	1080	0.45	22.29	4.17×10^{-3}	9.22×10^{-1}
TMA	389	16.42	528	840	0.34	16.76	4.05×10^{-3}	1.19×10^{0}
C/PA	414	0.87	546, 588	55	0.04	0.91	7.27×10^{-3}	18.2×10^{0}
C/IPA	413	17.64	515	285	1.70	19.34	1.67×10^{-2}	9.65×10^{-1}
C/TMA	416, 453	0.85	505	147	0.23	1.08	1.56×10^{-2}	6.79×10^{0}
CE/PA	430	0.18	491, 523	85	0.22	0.40	2.59×10^{-2}	11.7×10^{0}
CE/IPA	413	3.74	488, 519	311	4.96	8.70	1.59×10^{-1}	3.06×10^{0}
CE/TMA	428	0.80	486, 518	176	2.16	2.96	1.23×10^{-1}	5.56×10^{0}
CCA/PA	419	0.66	488, 522	60	0.57	1.23	9.50×10^{-2}	16.6×10^{0}
CCA/IPA	417	5.20	481, 518	327	2.85	8.05	8.72×10^{-2}	2.97×10^{0}
CCA/TMA	408	4.99	482, 515	211	4.11	9.10	1.95×10^{-1}	4.54×10^{0}

[a] Doping concentrations of different materials were PA, IPA, TMA and optimal concentration of Cums/Ar-COOH doped material.

[b] Excitation wavelength.

[c] Fluorescence emission wavelength.

[d] Fluorescence quantum yield.

[e] Phosphorescence emission wavelength.

[f] Phosphorescence lifetime at room temperature.

[g] Phosphorescence quantum yield.

[h] Photoluminescence quantum yield.

[i] k_p is the radiative rate constant, $k_p = \phi_p / \tau_p$.

[j] k_{nr} is the nonradiative rate constant of the T_1 state, $k_{nr} = (1-\phi_p)/\tau_p$.

Table S2. SOC (ξ) for C, CE, and CCA monomer.

	SOC (ξ/cm^{-1})		SOC (ξ/cm^{-1})		SOC (ξ/cm^{-1})
C Monomer		**CE** Monomer		**CCA** Monomer	
$S_0 \rightarrow T_1$	1.2653	$S_0 \rightarrow T_1$	1.3700	$S_0 \rightarrow T_1$	0.7972
$S_1 \rightarrow T_1$	1.8935	$S_1 \rightarrow T_1$	20.677	$S_1 \rightarrow T_1$	14.233
$S_1 \rightarrow T_2$	1.1519	$S_1 \rightarrow T_2$	2.5818	$S_1 \rightarrow T_2$	3.5298
$S_1 \rightarrow T_3$	15.751	$S_1 \rightarrow T_3$	2.3980	$S_1 \rightarrow T_3$	1.2964
$S_1 \rightarrow T_4$	1.3176	$S_1 \rightarrow T_4$	6.4617	$S_1 \rightarrow T_4$	17.469
$S_1 \rightarrow T_5$	0.7754	$S_1 \rightarrow T_5$	10.120	$S_1 \rightarrow T_5$	10.025
$S_1 \rightarrow T_6$	1.0449	$S_1 \rightarrow T_6$	15.762	$S_1 \rightarrow T_6$	21.922
$S_1 \rightarrow T_7$	0.4428	$S_1 \rightarrow T_7$	7.9897	$S_1 \rightarrow T_7$	5.9417
$S_1 \rightarrow T_8$	1.4386	$S_1 \rightarrow T_8$	8.4718	$S_1 \rightarrow T_8$	2.8195
$S_1 \rightarrow T_9$	1.9178	$S_1 \rightarrow T_9$	3.7227	$S_1 \rightarrow T_9$	2.0304
$S_1 \rightarrow T_{10}$	0.8807	$S_1 \rightarrow T_{10}$	2.9976	$S_1 \rightarrow T_{10}$	0.4616
$S_1 \rightarrow T_{11}$	4.2745	$S_1 \rightarrow T_{11}$	11.915	$S_1 \rightarrow T_{11}$	3.3433
$S_1 \rightarrow T_{12}$	19.239	$S_1 \rightarrow T_{12}$	2.7073	$S_1 \rightarrow T_{12}$	8.5214
$S_1 \rightarrow T_{13}$	0.7273	$S_1 \rightarrow T_{13}$	1.0846	$S_1 \rightarrow T_{13}$	8.7758
$S_1 \rightarrow T_{14}$	1.2492	$S_1 \rightarrow T_{14}$	3.2929	$S_1 \rightarrow T_{14}$	6.0224
$S_1 \rightarrow T_{15}$	3.3013	$S_1 \rightarrow T_{15}$	3.6434	$S_1 \rightarrow T_{15}$	0.8708
$S_1 \rightarrow T_{16}$	1.7153	$S_1 \rightarrow T_{16}$	10.939	$S_1 \rightarrow T_{16}$	2.0735
$S_1 \rightarrow T_{17}$	0.2416	$S_1 \rightarrow T_{17}$	17.130	$S_1 \rightarrow T_{17}$	10.116
$S_1 \rightarrow T_{18}$	2.9318	$S_1 \rightarrow T_{18}$	23.445	$S_1 \rightarrow T_{18}$	5.1432
$S_1 \rightarrow T_{19}$	0.2734	$S_1 \rightarrow T_{19}$	5.7771	$S_1 \rightarrow T_{19}$	12.973
$S_1 \rightarrow T_{20}$	6.7909	$S_1 \rightarrow T_{20}$	10.063	$S_1 \rightarrow T_{20}$	3.9781